Radar Target Recognition by Machine Learning of K-Nearest Neighbors Regression on Angular Diversity RCS

Kun-Chou Lee

Department of Systems and Naval Mechatronic Engineering
National Cheng-Kung University, Tainan, 701, Taiwan
kclee@mail.ncku.edu.tw

Abstract ─ In this paper, the radar target recognition is given by machine learning of K-NN (K-nearest neighbors) regression on angular diversity RCS (radar cross section). The bistatic RCS of a target at a fixed elevation angle and different azimuth angles are collected to constitute an angular diversity RCS vector. Such angular diversity RCS vectors are chosen as features to identify the target. Different RCS vectors are collected and processed by the K-NN regression. The machine learning belongs to the scope of artificial intelligence, which has attracted the attention of researchers all over the world. In this study, the K-NN rule is extended to achieve regression and is then applied to radar target recognition. With the use of K-NN regression, the radar target recognition is very simple, efficient, and accurate. Numerical simulation results show that our target recognition scheme is not only accurate, but also has good ability to tolerate random fluctuations.

Index Terms ─ Machine learning, radar cross section, radar target recognition.

I. INTRODUCTION

Radar target recognition means to identify a target from features of electromagnetic signals. It plays a very important role in both military detection and non-destructive testing. There have been many techniques of radar target recognition. The electromagnetic imaging [1-3], i.e., inverse scattering, is the most direct approach for identification. However, this is often practically difficult because the phase information of the scattered electric field is required [1-2] and is difficult in measurement. Theoretically, the electromagnetic imaging requires rigorous numerical procedures of solving integral equations which are complicated and time-consuming [3]. Note that the efficiency is very important for practical target recognition. In [4], the radar target recognition is successfully achieved by using pattern recognition techniques [5] on RCS (radar cross section) [6]. Practically, measurement of RCS is easier than that of electric field phase. Moreover, the pattern recognition computation is easier than that of inverse scattering.

Recently, machine learning [7] has attracted interest of researchers in different fields all over the world. Machine learning belongs to the scope of artificial intelligence. It teaches a computer to predict the response of a system by learning from experiences. The goal is to build an intelligent system. A machine learning technique is basically a black box, which can achieve both pattern recognition and regression. The term "black box" means that the relation between the input and output of a system is very complex. This study plans to predict the type of a target from scattered RCS. The relation between the target's information and its RCS is complicated and strongly nonlinear. Therefore, machine learning is a good candidate for radar target recognition, e.g., [8-10].

In this paper, the radar target recognition is given by machine learning of K-NN (K-nearest neighbors) [11-14] regression [15] on angular diversity RCS. The K-NN algorithm is a fundamental machine learning algorithm. It is a non-parametric method used for both classification [11-14] and regression [15]. In both cases, the input consists of the K closest training examples in the feature space and the output is predicted accordingly. Similar to [4], the bistatic RCS of a target at a fixed elevation angle and different azimuth angles are collected to constitute an angular diversity RCS vector. Such angular diversity RCS vectors are chosen as features to identify the target. The target recognition procedures are divided into two stages, which are off-line (training) and on-line (predicting). In the off-line (training) stage, different RCS vectors from reference (known) targets are collected to constitute the RCS signal map. In the on-line (predicting) stage, an angular diversity RCS vector from an unknown target is detected. This on-line RCS vector is compared with the off-line RCS signal map by K-NN regression to identify the unknown target. With the use of K-NN regression, the radar target recognition is very simple and efficient. Numerical simulation results show that our target recognition scheme is not only accurate, but also has good ability to tolerate random fluctuations.

Submitted On: September 21, 2017
Accepted On: December 24, 2018

II. RCS COLLECTION

As a target is illuminated by an electric field $\bar{E}_i$, a current $\bar{J}$ will be induced and this current will then radiate a scattered electric field $\bar{E}_S$ as [16],

$$\bar{E}_S(\bar{r}) = -j\omega\mu_0 \int_{V'} \bar{\bar{G}}(\bar{r}-\bar{r}') \cdot \bar{J}(\bar{r}')dV' . \quad (1)$$

In (1), ω is the angular frequency, μ_0 is the permeability, $\bar{r}$ represents the location, and V' represents the target body. Note that the notation prime denotes the source region. The $\bar{\bar{G}}$ is the dyadic Green's function as [16],

$$\bar{\bar{G}}(|\bar{r}-\bar{r}'|) = \left(\bar{\bar{I}} + \frac{\nabla\nabla}{k_0^2}\right)\frac{e^{-jk_0|\bar{r}-\bar{r}'|}}{4\pi|\bar{r}-\bar{r}'|}, \quad (2)$$

where k_o is the wavenumber and $\bar{\bar{I}}$ is the identity matrix. By using numerical techniques, e.g., moment methods [17], and boundary conditions on (1), the induced current $\bar{J}$ and then the scattered electric field $\bar{E}_S$ can be calculated accordingly.

Without loss of generality, this study selects the ship-shaped scatterer as the target for simplicity. Consider a ship-shaped target on the sea level (*X*-*Y* plane) located at the origin of coordinate, as shown in Fig. 1. The front end of the ship is in the $+\hat{x}$ direction and the broadside of the ship is in the $\pm\hat{y}$ directions.

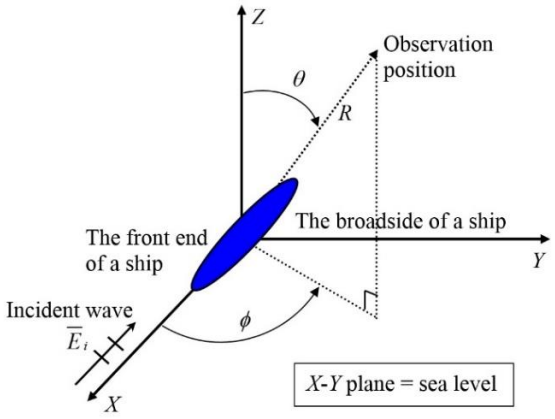

Fig. 1. Schematic diagram of a ship-shaped target illuminated by an incident plane wave.

The spherical coordinate system is defined as (R,θ,ϕ) where R is the distance from observation position to origin, θ is the elevation angle and ϕ is the azimuth angle. The target is illuminated by a $\hat{z}$-polarized plane wave $\bar{E}_i$. The bistatic RCS in the direction of (θ,ϕ) is defined as [6],

$$RCS(\theta,\phi) = \lim_{R\to\infty} 4\pi R^2 \frac{\left|\bar{E}_S(\theta,\phi)\right|^2}{\left|\bar{E}_i\right|^2}, \quad (3)$$

where $\bar{E}_S(\theta,\phi)$ is given in equation (1). The bistatic RCS data of a ship at a fixed elevation angle θ and different azimuth angles of ϕ are collected to constitute an RCS vector. This is just the angular-diversity RCS because measurement is taken by sweeping the spatial angles. Such angular-diversity RCS vectors are chosen as features to identify the target. Different RCS vectors are collected and processed by the K-NN regression of the next section.

III. K-NN REGRESSION

The K-NN (K-nearest neighbors) rule is first proposed by Cover & Hart [11] for classification. The basic concept of K-NN rule is very simple [11-14]. Figure 2 illustrates the K-NN rule for two categories. In Fig. 2, there are many known objects, which are blue triangles (label #1) and red rectangles (label #2), from two categories. Note that the label is an integer to represent a category. The problem is to predict which category a new unknown object (green circle) belongs to. In classical K-NN rule [11-14], a new object is classified by a majority vote of its neighbors. In other words, a new object is assigned to the category which is the most common among its *K* nearest neighbors. In Fig. 2, the solid contour line represents *K*=3 because it surrounds three known objects, which are one blue triangle (label #1) and two red rectangles (label #2). Thus, we predict that the new unknown (green) object belongs to the category of red rectangles (label #2). Similarly, the dash contour line represents *K*=5 because it surrounds five known objects, which are three blue triangles (label #1) and two red rectangles (label #2). Thus, we predict that the new unknown (green) object belongs to the category of blue triangles (label #1).

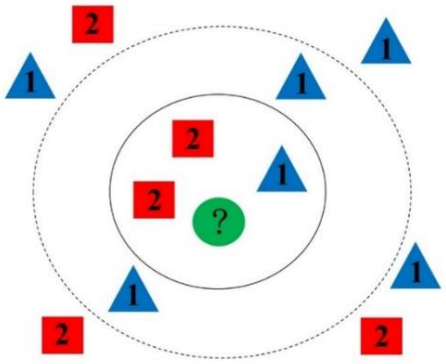

Fig. 2. Illustration of the K-nearest neighbors rule for two categories.

The above classical K-NN rule can be further extended to achieve regression [15]. In K-NN regression, the output is a continuous real number, but not an integer, to represent the property value of an object. This property value can be calculated from the weighted average on the property values of its K nearest neighbors. The procedures are divided into two stages, which are off-line (training) and on-line (predicting). For convenience, each object in Fig. 2 is viewed as a vector. In the off-line (training) stage, there are N known vectors $\bar{r}_i$ (i = 1, 2, ⋯, N) from different M categories (labeled as #1, #2, ⋯, #M). Each vector $\bar{r}_i$ (i = 1, 2, ⋯, N) has a property value $q_i \in \{1, 2, \cdots, M\}$ to represent which category $\bar{r}_i$ belongs to. Note that $\bar{r}_i$ and q_i (i = 1, 2, ⋯, N) are known off-line data. In the on-line (predicting) stage, there is a new vector $\bar{r}$. The problem is to predict the property value for this new vector $\bar{r}$. Among the N known objects, assume the K nearest neighbors (with respect to the new vector $\bar{r}$) have vectors $\bar{\alpha}_k$ and corresponding property values β_k, where k = 1, 2, ⋯, K. The property value for this new vector $\bar{r}$ is predicted as:

$$q = \sum_{k=1}^{K} w_k \beta_k , \tag{4}$$

and

$$w_k = \frac{1/d(\bar{r}, \bar{\alpha}_k)}{\sum_{k=1}^{K} [1/d(\bar{r}, \bar{\alpha}_k)]} , \tag{5}$$

where $d(\cdot)$ represents the Euclidean distance between two vectors. Equation (5) means that the weight (i.e., impact) of a neighbor is proportional to the reciprocal of distance. That is, near neighbors have larger impact, and vice versa. The parameter K is a user-defined parameter. The result of equation (4) is the K-NN regression.

In this study, components of a vector represent the RCS data collected at different azimuth angles under the same elevation angle, i.e., an angular diversity RCS vector. Vectors of the same category mean the RCS vectors scattered from the same type of target. Off-line training vectors are the RCS data from reference (known) targets. The property value represents the type of a target. The new vector $\bar{r}$ represents the on-line RCS data scattered from an unknown target. Note that the predicted property value q in equation (4) is a real number, but not an integer. Taking the integer that is the closest to q, the resulting integer is just the predicted label (i.e., type) of the unknown target.

IV. NUMERICAL RESULTS

In this section, numerical examples are given to illustrate the above formulations. To easily obtain the scattering RCS data, all targets are assumed to be ship-shaped models. There are three types of reference (known) targets (M=3) including type #1 (to simulate a ship of container vessel), type #2 (to simulate a naval ship) and type #3 (to simulate a fishing boat). The geometrical models for the three types of reference (known) targets are shown in Fig. 3. The ship length a is chosen as $k_o a$ = 9.4 for the reference target of type #1, $k_o a$ = 6.3 for the reference target of type #2, and $k_o a$ = 3.1 for the reference target of type #3. All targets are laid on a rough seawater surface (X-Y plane). The seawater has dielectric constant ε_r = 81 and conductivity σ = 4 S/m. The characteristic for surface roughness of the seawater is assumed to be:

$$z(x, y) = \frac{4}{75} a \cdot \sin(\frac{15\pi}{4} x) \sin(\frac{15\pi}{4} y) + \frac{8}{75} a \cdot \tag{6}$$

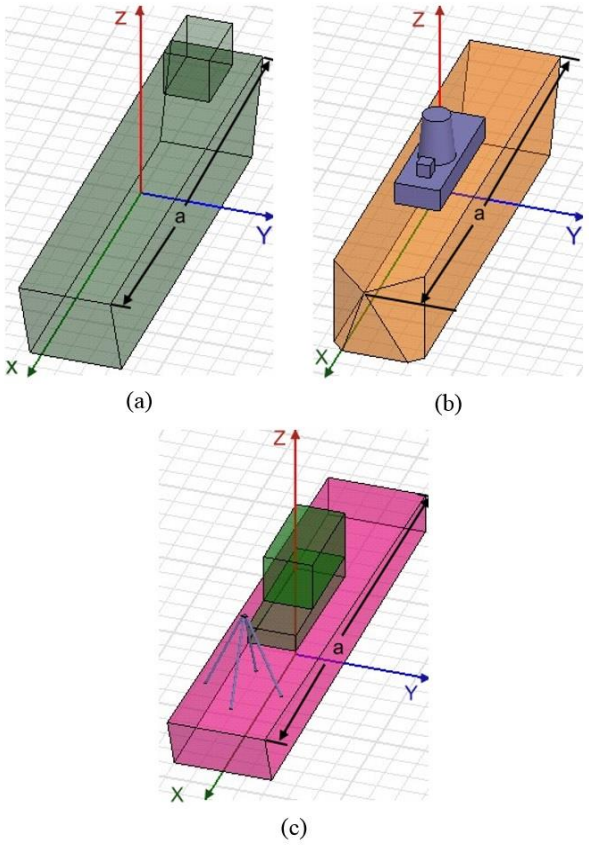

Fig. 3. Geometrical models for the three types of reference (known) targets: (a) type #1, (b) type #2, and (c) type #3.

The arrangement of RCS collection is illustrated in Fig. 1. Initially, the bistatic RCS data from the reference target of type #1 at the elevation angle θ= 61° and azimuth angles ϕ = 0°, 1°, …, 180°, are collected to constitute a 181-dimensional RCS vector, i.e., an angular diversity RCS vector. Next, the elevation angle θ is

changed to be $\theta = 63^o$, 65^o, …, and 89^o, respectively. Thus, we have 15 training vectors for the reference target of type #1. Similarly, the reference targets of type #2 and type #3 both have 15 training vectors. Therefore, we have 45 (N = 15×3) training vectors in total.

The RCS is simulated by the commercial software Ansys HFSS. Initially, the operation of Ansys HFSS software is verified. The bistatic RCS from a perfectly conducting sphere centered at the coordinate origin is computed by the Ansys HFSS software. The dimension of the perfectly conducting sphere is chosen to be $k_o b$ =1.1 and $k_o b$ =7.7 (b is the sphere radius) so that the results of RCS by Ansys HFSS software can be compared with those of reference [6] under the same parameters. Our simulation results show they are consistent. Thus, we conclude that our operation of Ansys HFSS software is correct. Next, the Ansys HFSS software is utilized to compute the RCS data in this study. Figure 4 shows the distribution of trained RCS data for the three known ships. The two horizontal axes represent the azimuth (ϕ) and elevation (θ) angles, respectively. The vertical axis represents the RCS. It shows that one cannot categorize these RCS data by visual inspection directly. Therefore, our K-NN identification is meaningful.

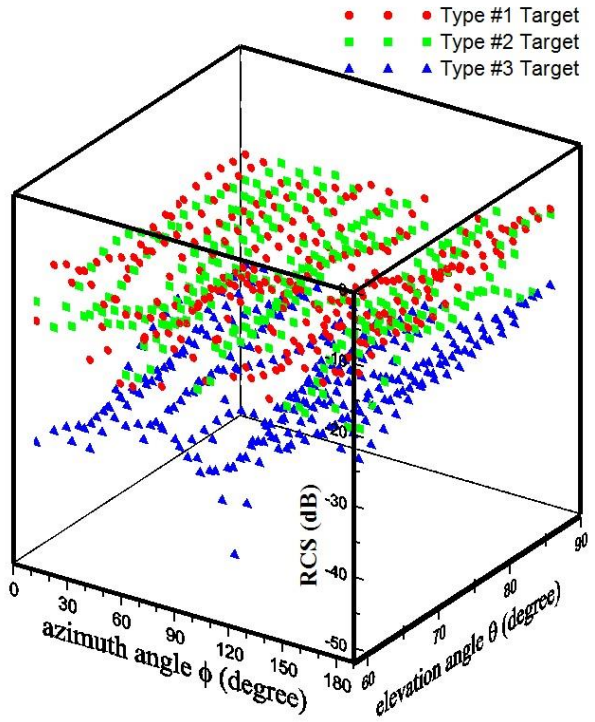

Fig. 4. Distribution of trained RCS data for the three known ships.

There are three examples to verify the above target recognition scheme. In the first example, the testing (unknown) target is the reference target of type #1. The RCS data are collected at the elevation angle $\theta = 62^o$ and azimuth angles ϕ = 0^o, 1^o, …, 180^o. Note that this elevation angle is different from any elevation angle of training RCS data. The goal is to predict the type of the testing (unknown) target by comparing on-line RCS data at $\theta = 62^o$ to training (i.e., off-line) RCS data. Following the K-NN regression rule in Section III, the predicted property value in equation (4) is q=1.048. Taking the integer that is the closest to q, the result is 1. Thus, we predict that the on-line RCS data at $\theta = 62^o$ are scattered from reference target of type #1. That is, we predict that the testing (unknown) target is just the reference target of type #1. This is consistent with the fact. Therefore, this is a correct prediction. Next, the elevation angle θ is changed to be $\theta = 64^o$, 66^o, …, and 90^o, respectively. Note that none of these elevation angles are included in elevation angles of training RCS data. Figure 5 shows the predicted property value, i.e., q of equation (4), for the 15 testing elevation angles at θ = 62^o, 64^o, …, and 90^o, respectively. Taking the integer that is the closest to q, the result is 1 for each test. Thus, we predict that the on-line RCS data at these 15 testing elevation angles are all scattered from the reference target of type #1. All predictions are correct and consistent with the fact. The successful recognition rate is 100% (=15/15).

In the second example, the testing (unknown) target is the reference target of type #2. The other conditions and procedures are the same as those of the first example. Figure 6 shows the predicted property value, i.e., q of equation (4), for the 15 testing elevation angles at θ = 62^o, 64^o, …, and 90^o, respectively. Taking the integer that is the closest to q, the result is 2 for each test. Thus we predict that the on-line RCS data at these 15 testing elevation angles are all scattered from the reference target of type #2. All predictions are correct and consistent with the fact. The successful recognition rate is 100% (=15/15).

In the third example, the testing (unknown) target is the reference target of type #3. The other conditions and procedures are the same as those of the first and second examples. The results are shown in Fig. 7. Taking the integer that is the closest to q, the result is 3 for each test. Thus, we predict that all on-line RCS data are scattered from the reference target of type #3. All predictions are correct and consistent with the fact. The successful recognition rate is 100% (=15/15).

The overall successful recognition rate is 100% (=45/45). All the above RCS data are from numerical simulation but not experiments. So, the RCS data are deterministic without random fluctuations. In practical applications, the experimental data contains random fluctuations such as interferences and noises. To investigate such effects, we add an independent random component to each RCS. This random component is with

Gaussian distribution and zero mean. The normalized standard derivation (with respect to the root mean square value of the RCS) is chosen as 0.01, 0.1, 0.2, 0.4, 1.0, 1.2, 1.4, 1.6, 1.8, and 2.0, respectively. Figure 8 shows the successful recognition rate with respect to different levels of added random components. For comparison, the results of reference [4], which utilizes PCA (principal components analysis) techniques [5], are also given. It reports that the successful recognition rate of this study is obviously better than that of reference [4] (using PCA). This study can still maintain the successful recognition rate of 75.56% even though the normalized standard derivation of the added random component is increased to 2. This result shows that the proposed target recognition scheme has good ability to tolerate random fluctuations.

In the above simulation, our ocean surface model of equation (6) is somewhat too simple. Many complex scattering mechanisms of the actual ocean, e.g., the Bragg scattering, are not included in our ocean surface model. However, this will not degrade the effectiveness of our K-NN target recognition. From Fig. 8, it reports that our recognition can still maintain the successful recognition rate of 75.56% even though the normalized standard derivation of the added random component is increased to 2. The complex scattering mechanism of the actual ocean may be viewed as one of the sources for the added random component in Fig. 8. This implies that our recognition is still available although there exists complex scattering mechanisms of the actual ocean.

The above RCS is computed by the Ansys HFSS software on a personal computer. The other processing is coded using Python-3.6 programming language in Anaconda software. The hardware is a personal computer with Intel(R) Core(TM) i7-4790 3.6 GHz CPU and 16 GB RAM.

V. CONCLUSION

This study successfully utilizes machine learning of K-NN regression to implement radar target recognition. With the use of K-NN regression, the recognition procedure is simple and accurate with good discrimination. Numerical simulation results show that the recognition scheme has good ability to tolerate random fluctuations. Unlike mathematical regression, the K-NN regression is inherently a black box. It can model a very complicated system and can be applied to many complicated and nonlinear problems of electromagnetic waves. It should be noted that our recognition has no limitation on the number of categories. As the number of categories increases, the flowchart of our target recognition is still unchanged. Like most schemes of radar target recognition, the successful rate of identification will be challenged as the RCS difference becomes smaller. Under such situations, the RCS data should be processed in advance for reducing the fluctuating components. For example, the SVD (singular value decomposition) technique [18-19] can decompose a noisy signal into clean and noisy components by mapping signals to matrix subspace. Using only the clean RCS to implement our K-NN target recognition may improve the discrimination. This will be the future work of this study.

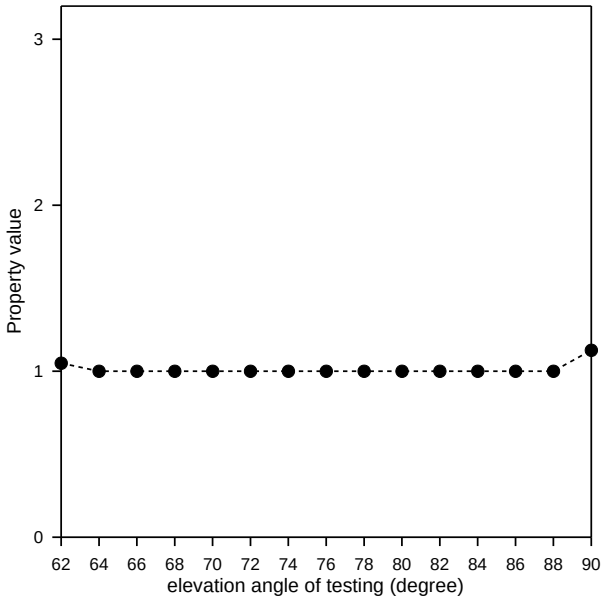

Fig. 5. Predicted property value for different elevation angles of testing as the target is the reference target of type #1.

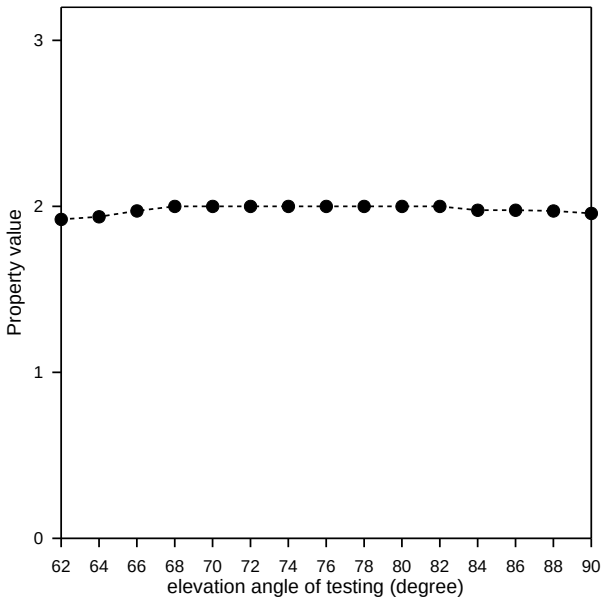

Fig. 6. Predicted property value for different elevation angles of testing as the target is the reference target of type #2.

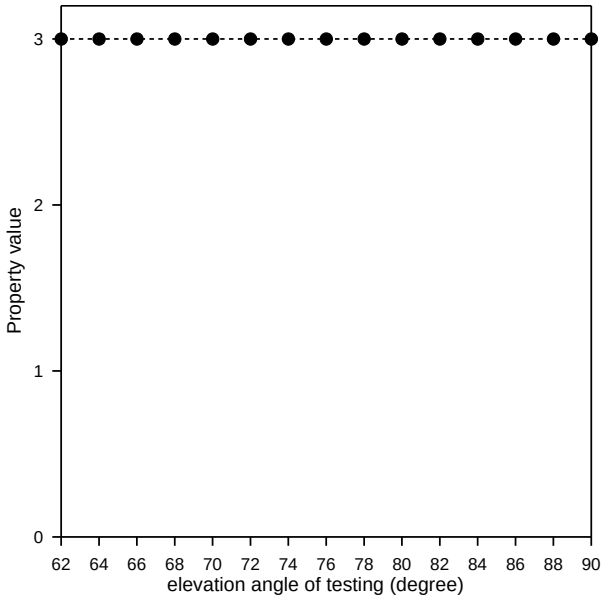

Fig. 7. Predicted property value for different elevation angles of testing as the target is the reference target of type #3.

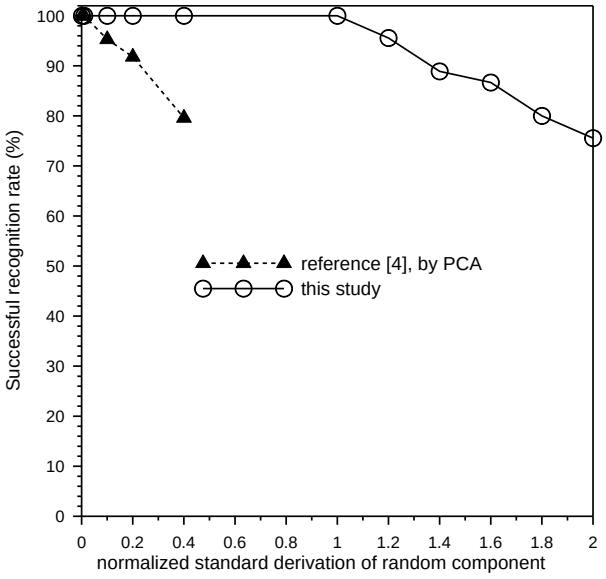

Fig. 8. Successful recognition rate with respect to different levels of added random components.

ACKNOWLEDGMENT

The authors would like to acknowledge (1) the financial support of the Ministry of Science and Technology, Taiwan, under Grant MOST 107-2221-E-006-098, (2) the National Center for High Performance Computing, Taiwan, for computer time and facilities.

REFERENCES

[1] N. H. Farhat, "Microwave diversity imaging and automated target identification based on models of neural networks," *Proc. IEEE*, vol. 77, no. 5, pp. 670-681, 1989.

[2] K. C. Lee, "Polarization Effects on Bistatic Microwave Imaging of Perfectly Conducting Cylinders," *Master Thesis*, National Taiwan University, Taipei, Taiwan, 1991.

[3] K. C. Lee, "Inverse scattering of a conducting cylinder in free space by modified fireworks algorithm," *Prog. Electromagn. Res. M*, vol. 59, pp. 135-146, 2017.

[4] K. C. Lee, J. S. Ou, and C. W. Huang, "Angular-diversity radar recognition of ships by transformation based approaches --- including noise effects," *Prog. Electromagn. Res.*, vol. 72, pp. 145-158, 2007.

[5] S. Theodoridis and K. Koutroumbas, *Pattern Recognition*. 2nd ed., Academic Press, Boston, 2003.

[6] G. T. Ruck, D. E. Barrick, W. D. Stuart, and C. K. Krichbaum, *Radar Cross Section Handbook*. vol. 1, Plenum, New York, 1970.

[7] S. Suthaharan, *Machine Learning Models and Algorithms for Big Data Classification*. Springer, New York, 2016.

[8] S. Caorsi, D. Anguita, E. Bermani, A. Boni, M. Donelli, and A. Massa, "A comparative study of NN and SVM-based electromagnetic inverse scattering approaches to on-line detection of buried objects," *Appl. Comput. Electromagn. Soc. J.*, vol. 18, no. 2, pp. 1-11, 2003.

[9] A. Kabiri, N. Sarshar, and K. Barkeshli, "Application of neural networks in the estimation of two-dimensional target orientation," *Appl. Comput. Electromagn. Soc. J.*, vol. 18, no. 2, pp. 57-63, 2003.

[10] D. Shi and Y. Gao, "Electromagnetic radiation source identification based on spatial characteristics by using support vector machines," *Appl. Comput. Electromagn. Soc. J.*, vol. 32, no. 2, pp. 120-127, 2017.

[11] T. M. Cover and P. E. Hart, "Nearest neighbor pattern classification," *IEEE Trans. Inf. Theory*, vol. IT-13, no. 1, pp. 21-27, 1967.

[12] P. E. Hart, "The condensed nearest neighbor rule," *IEEE Trans. Inf. Theory*, vol. IT-14, no. 3, pp. 515-516, 1968.

[13] P. Hall, B. U. Park, and R. J. Samworth, "Choice of neighbor order in nearest neighbor classification," *Ann. Stat.*, vol. 36, no. 5, 2135-2152, 2008.

[14] I. Mesecan and I. Bucak, "Searching the effects of

image scaling for underground object detection using K-means and K-NN," *The 8th European Modelling Symposium (EMS)*, Pisa, Italy, pp. 180-184, Oct. 2014.

[15] N. S. Altman, "An introduction to kernel and nearest-neighbor nonparametric regression," *Am. Stat.*, vol. 46, no. 3, pp. 175-185, 1992.

[16] C. T. Tai, *Dyadic Green's Functions in Electromagnetic Theory*. International Textbook Company, San Francisco, 1971.

[17] R. F. Harrington, *Field Computation by Moment Methods*. Macmillan, New York, 1968.

[18] K. C. Lee, J. S. Ou, and M. C. Fang, "Application of SVD noise-reduction technique to PCA based radar target recognition," *Prog. Electromagn. Res.*, vol. 81, pp. 447-459, 2008.

[19] T. K. Moon, and W. C. Stirling, *Mathematical Methods and Algorithms for Signal Processing*. Prentice Hall, New Jersey, 2000.

Kun-Chou Lee was born in Taiwan. He received his B.S. degree in 1989, M.S. degree in 1991, and Ph.D. degree in 1995, from the National Taiwan University, Taipei, Taiwan, all in Electrical Engineering. From 1995 to 1997, he joined the army of his country. From 1997 to 2003, he joined the Faculty of the Wu-Feng Institute of Technology, Shu-Te University, and National Kaohsiung University of Applied Sciences, respectively, all in southern Taiwan. Since 2004, he has been with the Department of Systems and Naval Mechatronic Engineering, National Cheng-Kung University, Tainan City, Taiwan, where he is currently a Professor. His research interests include electromagnetic waves, signal processing and communications. He is a Senior Member of IEEE, and a Mmember of ACES.